Griffiths, D. V., Hicks, M. A. & Li, C. O. (1991). *Géotechnique* **41**, No. 4, 615–620

TECHNICAL NOTE

Transient passive earth pressure analyses

D. V. GRIFFITHS,* M. A. HICKS* and C. O. LI*

KEYWORDS: consolidation; dredging; earth pressure; numerical modelling and analysis; pore pressures; time dependence

INTRODUCTION

Many analyses of geotechnical problems assume that the soil is either fully drained or fully undrained. The validity of these assumptions depends to a large extent on the permeability of the soil, the drainage path lengths and the rate at which loads are applied. This Technical Note describes a finite element technique which takes account of transient effects through a Biot analysis, enabling coupling of the pore pressure variations to a non-linear soil stress–strain law. The algorithm, which can retrieve both drained and undrained solutions as special cases, is applied to a problem of passive earth pressure with variable wall speeds. This type of analysis has applications to dredging, in which the dilative tendency of the soil is shown to have a significant effect on its passive resistance. Related applications include offshore anchors and skirt-foundation systems of offshore gravity platforms.

In this Technical Note, the Biot (1941) formulation is used to study the coupled interactions between the solid and fluid phases. This approach, which treats the soil as a two-phase material, has been used successfully in several geotechnical applications, usually involving linear soil models (see for example Hwang, Morgenstern & Murray, 1971; Smith and Hobbs, 1976). Non-linear soil models have also been incorporated into the Biot formulation, for example by Small, Booker & Davis (1976) in analysing boundary value problems using an elastic–perfectly plastic Mohr–Coulomb constitutive law, and by Hicks and Smith (1986), who considered more complicated soil models.

TRANSIENT ANALYSIS INCORPORATING PLASTICITY

The non-linear soil behaviour is assumed to be elastic–perfectly plastic, and is modelled using a viscoplastic type of algorithm. Each time step of the transient behaviour is treated as a pseudo-static analysis, within which stresses that have violated the operating failure criteria are redistributed iteratively.

The Biot and viscoplastic formulations are described in detail elsewhere; the coding for both is given in full by Smith and Griffiths (1988). In this study, a fully implicit incremental formulation is used (see, e.g. Hicks, 1990). This leads to the matrix version of the Biot equations at the element level

$$\begin{bmatrix} k_m & c \\ c^T & -\Delta t \theta k_p \end{bmatrix} \begin{Bmatrix} \Delta r \\ \Delta \phi \end{Bmatrix} = \begin{Bmatrix} \Delta f \\ \Delta t k_p \phi_0 \end{Bmatrix} \quad (1)$$

where k_m is the element solid stiffness matrix, k_p is the element fluid 'stiffness' matrix, c is the element coupling matrix, Δr is the change in nodal displacements, $\Delta\phi$ is the change in nodal excess pore pressures, ϕ_0 is the 'old' nodal excess pore pressures, Δf is the change in nodal forces, Δt is the calculation time step and θ is the time stepping parameter ($=1$ in this work).

After assembly of the global equations, repeated solution of simultaneous equations is necessary. An advantage of using this approach rather than an explicit ($\theta = 0$) method is that the long-term or steady state solution can be achieved in a single large time step, provided that the left hand side matrix remains constant.

APPLICATION TO EARTH PRESSURE

The transient analyses were next applied to a problem of passive earth pressure. The practical applications of such a study relate to the dredging process, whereby underwater soils are removed by excavators in order to maintain sufficient depth in ports, harbours, rivers and canals. The choice of dredging equipment and the properties of the soil to be excavated are of prime importance, as they have a significant influence on the power required to remove the soil bed. A study on the soil mechanics aspects of dredging by van Leussen and Nieuwenhuis (1984) concluded that the dilative properties of the soil could be highly significant in an undrained or partially drained environment.

Other applications include the estimation of

Discussion on this Technical Note closes 1 April 1992; for further details see p. ii.

* Department of Engineering, University of Manchester.

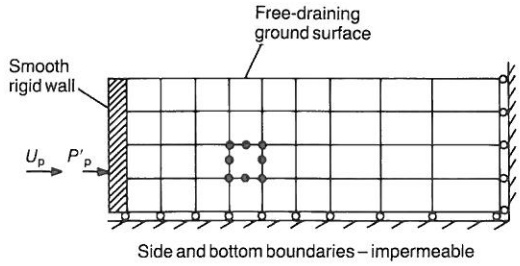

Fig. 1. Mesh used for earth pressure analyses: side and bottom boundaries impermeable

the holding capacity of anchors for ships and offshore structures. In such systems, the passive resistance of the saturated soil is directly relevant to the anchor capacity. Experimental and finite element studies of loaded anchor plates have been reported by Neely, Stuart & Graham (1973) and Rowe & Davis (1982), but assume that the soil is fully drained. The lateral soil resistance that can be mobilized by a skirt-foundation system of an offshore gravity platform during storm loading also relates to the transient analyses presented in this paper.

Influence of wall speed

The effect of wall speed on passive resistance of non-dilative soils is now considered. The plane strain mesh geometry is shown in Fig. 1. This simplified problem (see for example Crisfield, 1987) disregards the shear concentration that would normally be observed at the base of the wall, but does not detract from the analysis in the case of a smooth wall.

The excavation blade is idealized as a rigid vertical smooth wall translated horizontally into the soil bed. All boundaries of the mesh are impermeable except the top surface, at which drainage can occur. The mesh consists of eight-noded elements for the solid (soil) phase and four-noded elements for the fluid phase (Zienkiewicz, 1977). The soil is saturated, with shear strength defined by Mohr–Coulomb and parameters c' and ϕ'. Two-point Gaussian quadrature has been used throughout.

The soil is given the properties

$$E' = 1 \times 10^4 \text{ kPa}$$
$$\nu' = 0{\cdot}25$$
$$c' = 0 \text{ kPa}$$
$$\phi' = 30^\circ \ (K_p = 3)$$
$$\gamma' = 10 \text{ kN/m}^3$$
$$K_0 = 0{\cdot}5$$
$$k/\gamma_w = 1 \times 10^{-5} \text{ m}^4/\text{kN s}$$
$$c_v = 0{\cdot}12 \text{ m}^2/\text{s}$$

where γ' is the submerged unit weight and K_0 is the coefficient of earth pressure at rest. The wall is 1 metre high.

Computation of failure loads is the priority in the present work, so no attempt has been made to model soil deformations accurately. Although the value of Young's modulus attributed to the soil is arbitrary, it will be approximately inversely proportional to the computed deformations. Hence, if more realistic soil moduli were available the resulting deformations could be estimated by simple scaling.

A dimensionless dredging rate L_R is used to represent the (constant) speed of the wall as it moves into the soil. This quantity is defined as

$$L_R = \frac{\mathrm{d}(x/H)}{\mathrm{d}T_d} \tag{2}$$

with the time factor T_d given by

$$T_d = \frac{c_v t}{H^2} \tag{3}$$

and the coefficient of consolidation c_v by

$$c_v = \frac{k(1-\nu')E'}{\gamma_w(1-2\nu')(1+\nu')} \tag{4}$$

The height of the wall is H, and x represents the distance moved by the wall after time t.

Assuming a non-dilative soil ($\psi' = 0^\circ$), the distribution of horizontal effective stress and excess pore pressure adjacent to the wall are shown in Fig. 2 for three different dredging rates. All three parts of Fig. 2 give the stress state following a total wall displacement of 7·2 mm, which was achieved numerically using 60 equal increments. The calculation time steps were 0·001 s, 0·1 s and 10 s respectively for the fast, intermediate and slow cases.

At the fast dredging rate ($L_R = 1{\cdot}0$), the soil behind the wall behaves in an undrained manner, whereas at the slow dredging rate ($L_R = 0{\cdot}0001$) drained conditions are approximated. An intermediate response is observed at the compromise dredging rate ($L_R = 0{\cdot}01$).

In the undrained case, analytical solutions (Griffiths, 1985; Li, 1988) for the horizontal effective stress σ_x' and excess pore pressure Δu at depth z adjacent to the wall in a non-dilating soil at failure are given by

$$(\sigma_x')_f = \frac{\gamma' z K_p(K_0+1)}{K_p+1} \tag{5}$$

$$(\Delta u)_f = \frac{\gamma' z(K_p-K_0)}{K_p+1} \tag{6}$$

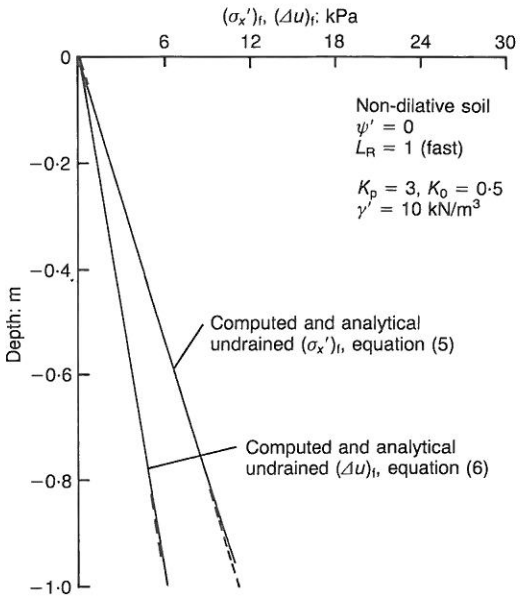

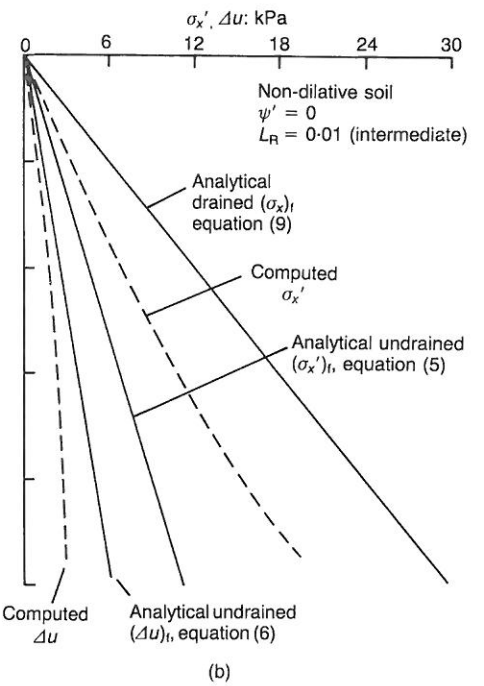

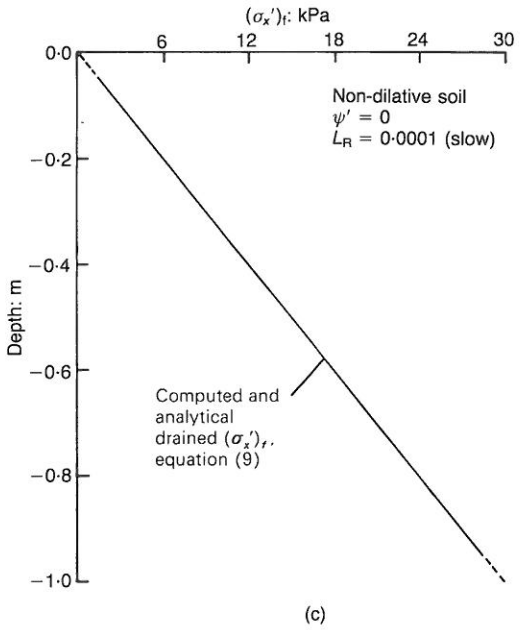

Fig. 2. Soil and water pressures at failure: (a) fast loading rate; (b) intermediate loading rate; (c) slow loading rate

which correspond to the net soil and excess pore water forces

$$P_p' = \frac{1}{2}\gamma' H^2 \frac{K_p(K_0 + 1)}{K_p + 1} \tag{7}$$

$$U_p = \frac{1}{2}\gamma' H^2 \frac{(K_p - K_0)}{K_p + 1} \tag{8}$$

In the drained case, the simple Rankine solution is obtained

$$(\sigma_x')_f = \gamma' z K_p \tag{9}$$

$$(\Delta u)_f = 0 \tag{10}$$

corresponding to the soil force

$$P_p' = \tfrac{1}{2}\gamma' H^2 K_p \tag{11}$$

The finite element results agree with these solutions, as shown in Fig. 2(a) for the fast wall (undrained) and Fig. 2(c) for the slow wall. For the intermediate wall, Fig. 2(b) shows the partially drained nature of the results. As expected, the computed pore pressures lie below the limit given by equation (6), and the effective stresses lie between the undrained and drained values given by equations (5) and (9) respectively.

The effective and excess pore water forces are computed by integrating the stresses in the column of elements adjacent to the wall. The sum of these reactions is plotted in dimensionless form in Fig. 3(a) (effective) and Fig. 3(b) (excess). As the soil model used in these analyses was non-dilative, the slow-moving wall (drained) led to greater passive resistance than the fast-moving wall (undrained), in which compressive pore pressures were generated. The computed drained and

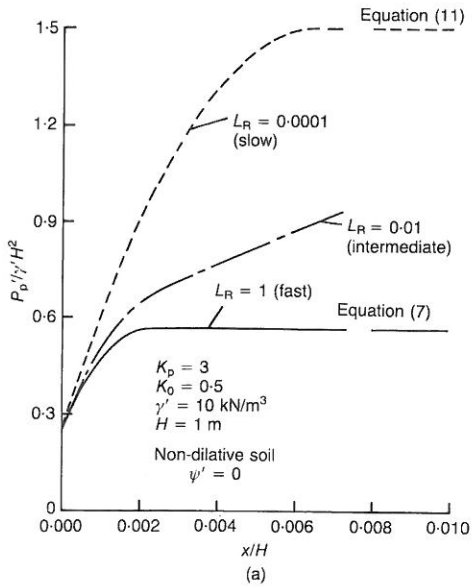

Fig. 3. Plots of: (a) effective force against displacement; (b) water force against displacement

undrained limit loads agree closely with closed form solutions deduced from equations (7) and (11).

Regarding the excess pore water forces shown in Fig. 3(b), the fast-moving wall gave close agreement with equation (8). In the case of intermediate rate of wall movement, the water force initially increases and then starts to fall as the pressures are redistributed.

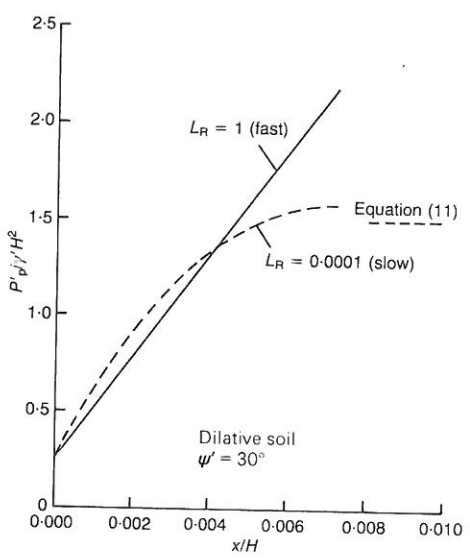

Fig. 4. Influence of wall speed on dilative soil

Influence of dilation angle

Figure 4 shows the effect of the dilation angle on the effective force behind the wall for the fast and slow cases. In the fast case, the effective force continues to rise well beyond the drained Rankine solution. In the slow case, the dilation angle makes virtually no difference to the solution, and the result converges on the drained solution given by equation (11).

In the present work, the dilation angle is constant; this is a deficiency of the simple model. In real soils, continuous shearing will reduce the rate of dilation until the critical state is reached, at which point soil continues to shear at constant volume and constant pore pressure (see e.g., Seed and Lee, 1967). The reduction of pore pressure is also limited in practice by cavitation.

The analysis was repeated for both the dilative and non-dilative soils with a variable wall speed. In this case the wall was initially moved at the fast rate for 60 increments of displacement, followed by 60 increments at the slow rate as shown in Fig. 5. The reason for the slow wall movement was to allow any excess pore pressures to drain away while still applying additional shear stresses to the soil.

The plots of the soil force against the wall are shown in Fig. 6(a). In the non-dilative soil, the effective force rapidly reaches its undrained limit value given by equation (7). Subsequent pore pressure dissipation during the slow period causes the pore pressures next to the wall to fall, and the shear strength of the soil to rise until the Rankine (drained) value is reached as given by equation

(11). In this case, the minimum passive resistance is achieved in the short term (undrained).

In the dilative soil, the effective force rises steeply at first, but during the 'slow' pore pressure dissipation results in rising pore pressures, and the shear strength of the soil gradually falls until the Rankine (drained) value is again reached. In this case, the minimum passive resistance is achieved in the long term (drained).

The plots of the excess pore water force are shown in Fig. 6(b). During fast loading, the water force in the non-dilative soil rapidly reaches the undrained limit given by equation (8) and temporarily remains at that value. The dilative soil shows an initial rise in pore pressure due to elastic compressibility, followed by a sudden fall in pressure as the dilative soil tries to expand. After reduction of the wall speed to the slow rate, both water forces tend to zero as drained conditions are established.

CONCLUSIONS

The influence of loading rate and soil dilation on the passive resistance of saturated soils was examined using a finite element technique. With reference to dredging of soils, it was shown that if the soil has a tendency for dilation during shear, a fast rate of excavation might be undesirable because the resulting passive resistance would be higher than the drained value. Conversely, a fast dredging rate would facilitate the excavation process in a non-dilative soil, because the generation of compressive pore pressures would lower the passive resistance to less than the drained value.

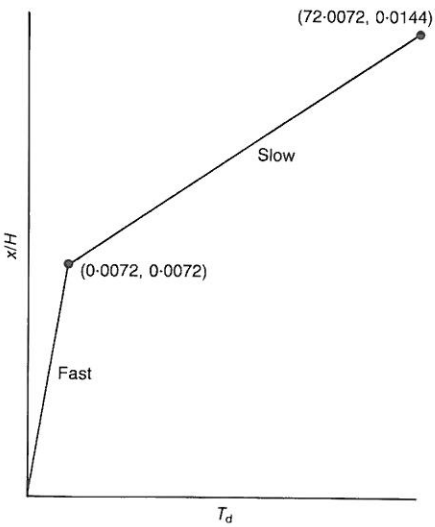

Fig. 5. Variable wall speed (not to scale)

With reference to other applications involving saturated soil: the holding capacity of an anchor or the soil resistance in a skirt-foundation system could be greatly enhanced by the dilative tendency of the soil in which it is embedded. If the soil is non-dilative, however, the holding capacity could be considerably reduced by compressive pore pressure generated during short-term loading events.

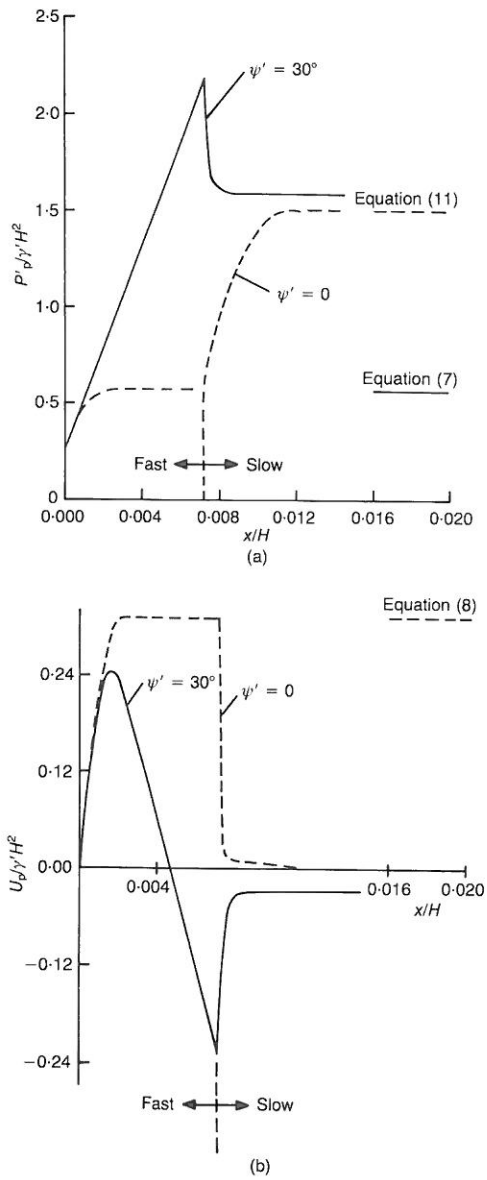

Fig. 6. Plots of: (a) effective force against displacement (variable wall speed); (b) water force against displacement (variable wall speed)

REFERENCES

Biot, M. A. (1941). General theory of three-dimensional consolidation. *J. Appl. Phys.* **12**, 155–164.

Crisfield, M. A. (1987). Plasticity computations using the Mohr–Coulomb yield criterion. *Engng Computations* **4**, No. 4, 300–308.

Griffiths, D. V. (1985). The effect of pore fluid compressibility on failure loads in elasto-plastic soils. *Int. J. Numer. Analyt. Meth. Geomech.* **9**, 253–259.

Hicks, M. A. (1990). *Numerically modelling the stress-strain behaviour of soils.* University of Manchester, PhD thesis.

Hicks, M. A. & Smith, I. M. (1986). Influence of rate of porepressure generation on the stress-strain behaviour of soils. *Int. J. Numer. Meth. Engng* **22**, No. 3, 597–621.

Hwang, C. T., Morgenstern, N. R. & Murray, D. W. (1971). On solutions of plane strain consolidation problems by finite element methods. *Can. Geotech. J.* **8**, 109–118.

Li, C. O. (1988). *Finite element analyses of seepage and stability problems in geomechanics.* University of Manchester, PhD thesis.

Neely, W. J., Stuart, J. G. & Graham, J. (1973). Failure loads of vertical anchor plates in sand. *J. Soil Mech. Fndn Engng Div., Am. Soc. Civ. Engrs*, **99**, No. SM9, 669–685.

Rowe, R. K. & Davis, E. H. (1982). The behaviour of anchor plates in sand. *Géotechnique* **32**, No. 1, 25–41.

Seed, H. B. & Lee, K. L. (1967). Undrained strength characteristics of cohesionless soils. *J. Soil Mech. Fndn Engng Div., Am. Soc. Civ. Engrs*, **93**, No. SM6, 333–360.

Small, J. C., Booker, J. R. & Davis, E. H. (1976). Elasto-plastic consolidation of soil. *Int. J. Solids & Struct.* **12**, 431–448.

Smith, I. M. & Griffiths, D. V. (1988). *Programming the finite element method* 2nd edn. New York: Wiley.

Smith, I. M. & Hobbs, R. (1976). Biot analysis of consolidation beneath embankments. *Géotechnique* **26**, 149–171.

van Leussen, W. & Nieuwenhuis, J. D. (1984). Soil mechanics aspects of dredging. *Géotechnique* **36**, 359–381.

Zienkiewicz, O. C. (1977). *The finite element method*, 3rd edn. London: McGraw Hill.